coatings

MDPI

Article

Electrochromic and Electrochemical Properties of Co_3O_4 Nanosheets Prepared by Hydrothermal Method

Xinrui Yue [1], Gang Wang [1], Jing Wang [1,*], Licai Fan [2], Jian Hao [3], Shen Wang [4], Mingli Yang [1] and Yang Liu [1]

[1] School of Light Industry, Harbin University of Commerce, Harbin 150028, China
[2] Beidahuang Information Co., Ltd., Harbin 150030, China
[3] State Key Laboratory of High-Efficiency Utilization of Coal and Green Chemical Engineering, Ningxia University, Yinchuan 750021, China
[4] School of Chemistry and Chemical Engineering, Quzhou College, Quzhou 324000, China
* Correspondence: wangwangmayong@126.com; Tel./Fax: +86-45184865185

Abstract: In this paper, Co_3O_4 nanosheets were prepared by the hydrothermal method. The structure of the material was analyzed by morphological characterization and physical phase analysis, which confirmed the preparation of the product, Co_3O_4, showing a nanosheet structure. By studying the electrochromic properties of the prepared products, the results show that the transmittance modulation range of the Co_3O_4 nanosheet is 75% at 780 nm. The coloring response time and bleaching response time is about 3.8 s and 3.4 s, respectively. Electrochemical tests show that the Co_3O_4 nanosheets have good capacitive properties. Their specific capacitance reaches 1850 F/g when the current density is 1 A/g. When the current density is 5 A/g, the specific capacitance can still maintain 99.6% after 5000 cycles. In addition, Co_3O_4//CNTs devices can provide a maximum energy density of 79.52 Wh/kg (1 A/g) and a maximum power density of 11,000 W/kg (15 A/g), showing good energy storage capacity. The above data results indicate that the prepared Co_3O_4 nanosheets can be used as good candidates for supercapacitors. This paper provides a new idea and method for preparing Co_3O_4 materials.

Keywords: Co_3O_4 nanosheets; hydrothermal method; electrically induced discoloration; supercapacitor

Citation: Yue, X.; Wang, G.; Wang, J.; Fan, L.; Hao, J.; Wang, S.; Yang, M.; Liu, Y. Electrochromic and Electrochemical Properties of Co_3O_4 Nanosheets Prepared by Hydrothermal Method. *Coatings* **2022**, *12*, 1682. https://doi.org/10.3390/coatings12111682

Academic Editors: Ajay Vikram Singh and Emerson Coy

Received: 22 September 2022
Accepted: 2 November 2022
Published: 5 November 2022

1. Introduction

With the rapid growth of energy demand and the continuous consumption of fossil fuels, today's society is facing more and more serious energy and environmental problems. In order to solve these problems, on the one hand, renewable and clean energy should be developed. Supercapacitors are usually used as energy storage devices for clean energy due to their excellent characteristics of high-power input and output and rapid charge and discharge [1]. On the other hand, to save energy, electrochromic materials can be widely used in buildings, vehicles, and other facilities to save energy by adjusting their own color and transmittance changes. Research and development with a variety of high-performance materials, to alleviate the energy crisis, has far-reaching significance [2,3].

Cobalt tetroxide is a P-type semiconductor, which has the advantages of high theoretical specific capacitance (over 3000 F/g), abundant reserves, low price, and environmental friendliness, and has been a hotspot for electrochemical performance research [4–7]. For example, Wang et al. [8] successfully prepared Co_3O_4 nanoparticles. At a high current density of 20 A/g, the specific capacitance retention rate is up to 99% with 10,000 cycles. Wang et al. [9] prepared the Co_3O_4 nanostructures on nickel foam. Under the condition of a scanning speed of 10 mV/s, the capacity of this electrode is 1090 F/g. Jahdaly et al. [10] successfully synthesized cobalt oxide nanoparticles by the hydrothermal method. The authors assembled it and the activated carbon (AC) as positive and negative electrodes, respectively, into devices. The asymmetric device has a current density of 1 A/g, a specific capacitance of 182 F/g, a maximum power density of 585 W/kg, and a maximum energy density of

25.27 Wh/kg. Conclusions regarding the above data provide a scientific basis for us to study the electrochemical properties of Co_3O_4 nanomaterials. In addition, cobalt tetroxide also has good electrochromic properties and a relatively short response time, which has attracted extensive attention from researchers. Wang et al. [11] prepared nanoporous Co_3O_4 films by electrodeposition, and the coloring response time and bleaching response time of the prepared nanoporous Co_3O_4 was 3.0 s and 2.6 s, respectively. Venkatesh et al. [12] successfully prepared Co_3O_4 thin films by spray pyrolysis. The film has a maximum light modulation of 35% and a coloring efficiency of 29 cm^2/C. Dhas et al. [13] successfully grew cobalt oxide (Co_3O_4) thin films on FTO using spray pyrolysis technology. The transmittance of the material reached 38.3%. Based on the above studies, it was found that Co_3O_4 nanomaterials have a wide range of research value in the material preparation and electrochromic field of supercapacitors.

In this paper, Co_3O_4 nanosheet materials with relatively good performance were prepared on nickel foam conductive substrates by the hydrothermal method. The data show that the material has good electrochemical and electrochromic properties, and the transmittance of the Co_3O_4 nanosheets at 780 nm is 25% and 100% in the colored and bleached states, respectively, with a modulation range of 75% for light transmission. In addition, the Co_3O_4 nanosheets are excellent electrode materials for supercapacitors. The specific capacitance was up to 1850 F/g at a current density of 1 A/g. The retention of specific capacitance was up to 99.6% after 5000 cycles. Finally, the Co_3O_4 nanosheets and CNTs were assembled into an asymmetric device, which can be stabilized with a potential window of 1.6 V and a specific capacitance of up to 339 F/g at 1 A/g. In addition, the device has a maximum energy density of 79.52 Wh/kg and a maximum power density of 11,000 W/kg.

2. Materials and Methods

2.1. Preparation of Co_3O_4 Nanosheets

The preparation steps of the Co_3O_4 nanosheets were as follows: Firstly, 0.2 g of PEO-PPO-PEO (Sate-polypropylene oxide-ate-oxide) and 13 g of ethanol were dissolved in 1 mL deionized water, and then magnetically stirred for 20 min to form the transparent solution A. Then, 0.125 g of $Co(Ac)_2{\cdot}4H_2O$ and 0.07 g of hexamethylenetetramine were added to solution A, and the purple solution B was obtained by magnetic stirring for 15 min. Secondly, 13 mL of ethylene glycol reagent was added to solution B, and the mixture was magnetically stirred for 30 min and placed at room temperature for 2 days. The nickel foam (size: $1 \times 1 \times 0.2$ cm^3) was cleaned with ethanol, acetone, and ultrapure water by ultrasonication for 10 min and then dried in the oven to obtain clean nickel foam. Clean nickel foam was placed in the solution and transferred to a 45 mL autoclave for 2 h at 170 °C. Then, the product was removed from the reactor and centrifuged for 20 min at 900 r/min. The black product was filtered out, washed three times (alternating between distilled water and ethanol), and dried at 80 °C for 24 h to obtain the precursor. Finally, the obtained precursor was placed in a Muffle furnace and heat treated for 0.5 h at 350 °C to obtain the brown powder, namely, the Co_3O_4 nanosheets.

2.2. Material Characterization

The microstructure and micromorphology of the prepared samples were characterized by scanning electron microscopy (SEM, JEOL-6360Lv, Tokyo, Japan) and transmission electron microscopy (TEM, JEOL JEM-201, Tokyo, Japan). The phase structure was analyzed using an X-ray diffractometer (Aolong Y2000, Dandong, China). A surface area and aperture analyzer (Tristar II, Micromeritics, Seoul, South Korea) was used to test the surface area and aperture data, respectively.

2.3. Electrochemical Performance Test and Preparation and Characterization of the Supercapacitor Devices

The electrochemical performance tests, device preparation, and characterization in this article are the same as in our previous articles. Please refer to the supporting information in our previous articles for more details [14]. The loading mass of Co_3O_4 was 2.9 mg cm^{-2} and those of the CNTs were 3.4 mg cm^{-2}. The specific capacitance, energy density, and power density after material testing are calculated as follows:

$$C_s = i\Delta t/m\Delta V \quad (1)$$

$$E = 0.5C_s\Delta V^2/3.6 \quad (2)$$

$$P = 3600E/\Delta t \quad (3)$$

$$m^+/m^- = C^- \times \Delta V^-/C^+ \times \Delta V^+ \quad (4)$$

where C_s is the specific capacity, i is the discharge current, t is the discharge time, ΔV is the voltage drop, m is the mass of the active material, E is energy density, and P is the power density.

2.4. Electrochromic Performance Testing

A three-electrode test system was carried out using a Co_3O_4 mold: a homogeneous layer of the polymer was plated on a conductive substrate; Co_3O_4/ITO was prepared as the working electrode, an Ag/Ag^+ electrode as the reference electrode, and Pt wire as the counter electrode; the electrolyte solution was a 0.1 M $LiClO_4$ solution. When testing the electrochemical properties of the absorption/transmission spectra, different voltages were applied to the electrodes in the amperometric I-t channel. To test the electrochromic stability properties at alternating square wave voltages, an alternating square wave voltage was applied with the chronoamperometry channel, and the absorbance-transmittance variation curves at set wavelengths were measured in situ inline with a UV-Vis-NIR spectrometer.

3. Results and Discussion

In order to observe the morphology and structure of the product, we carried out an SEM analysis of the product. Figure 1a is a low-magnification SEM image of Co_3O_4 nanomaterials grown on a foamed nickel conductive substrate. As can be seen in the figure, a large number of the Co_3O_4 nanomaterials were grown on a nickel foam conductive substrate. Figure 1b shows a high magnification SEM image of a Co_3O_4 nanosheet. There are a large number of nanosheets intertwined with each other in the figure, forming a mesh-like porous structure. The formed pores can provide convenient channels for the rapid migration and transfer of ions and electrons. To further confirm the elemental composition of the prepared product obtained, SEM mapping tests were carried out, as shown in Figure 1c,d. The results verified the presence of elemental Co and O, which indicated that the product did not contain other impurities. The above test results indicate that the synthesized product is a Co_3O_4 nanosheet material.

In order to observe the microscopic morphology of the product more closely, it was tested using transmission electron microscopy (TEM). The morphology of the Co_3O_4 nanosheets can be clearly observed according to Figure 2a. The average size of the nanosheets is 50 nm.We performed HRTEM at the red circle in Figure 2a, as shown in Figure 2b. It can be found that the crystal plane spacing is 0.28 nm, which corresponds to the (220) lattice of the Co_3O_4 material. As can be seen in the inset of Figure 2b, the SEAD test indicates a distinct diffraction ring, suggesting that the prepared Co_3O_4 material is polycrystalline. We further tested the elemental mapping of Co_3O_4 by energy dispersive spectroscopy (EDS). It can be seen in Figure 2c that the prepared Co_3O_4 nanomaterial contains both Co and O elements, which is consistent with the SEM mapping test. Figure 2d shows an X-ray diffraction (XRD) test of the material to analyze the physical phase structure of the Co_3O_4 nanosheets. The diffraction peaks in the figure are sharp and the presence

of other impurity peaks was not observed. All the diffraction peaks correspond to the standard diffraction card (PDF card no. 65-3103). All the above analyses indicate that the prepared material is Co_3O_4.

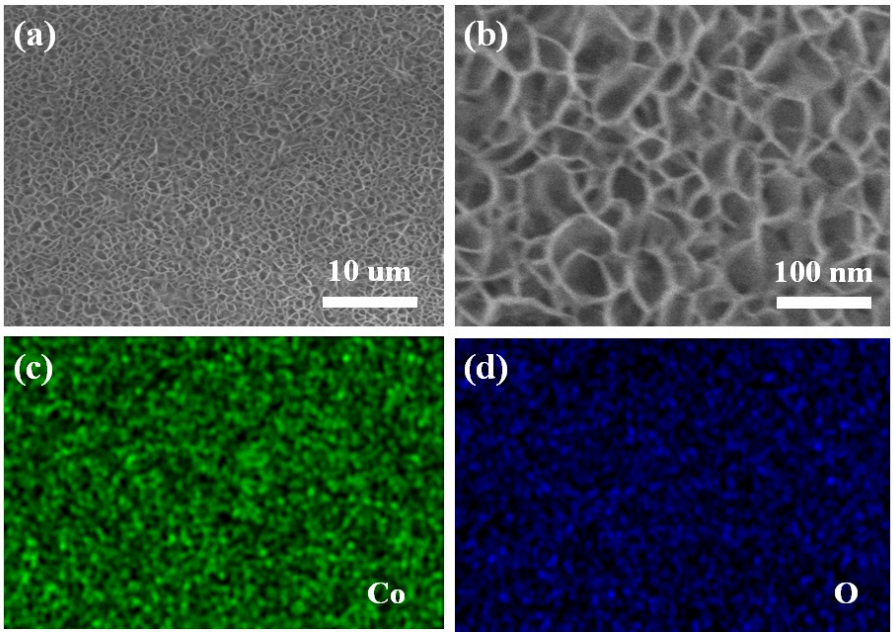

Figure 1. (**a**,**b**) SEM images of Co_3O_4 at different magnifications. (**c**,**d**) SEM mapping images of Co and O elements, respectively.

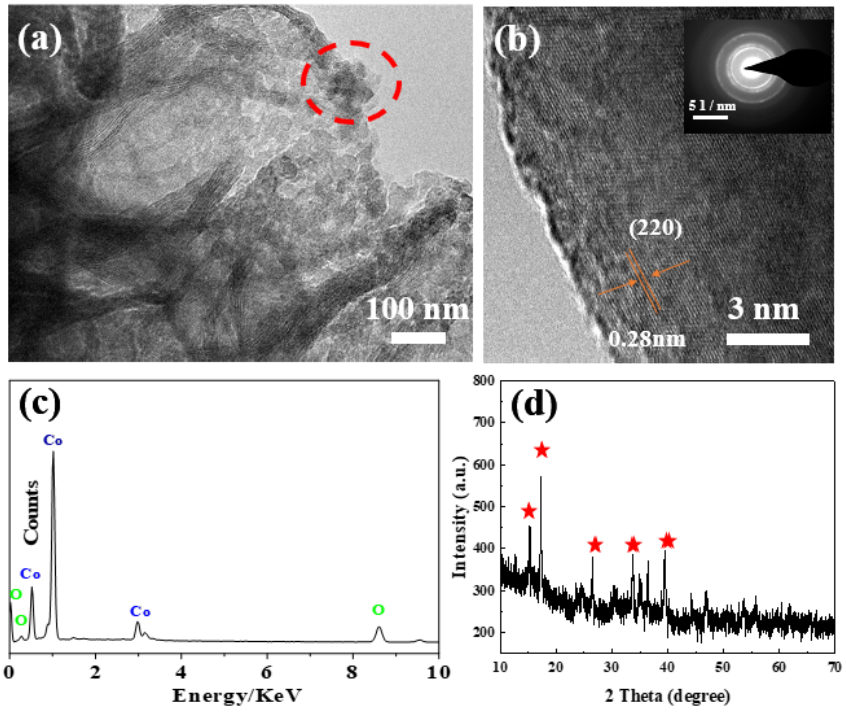

Figure 2. (**a**) TEM images of Co_3O_4 nanosheets. (**b**) HRTEM images of Co_3O_4 nanosheets. (**c**) EDS spectra of Co_3O_4 nanoparticles. (**d**) XRD spectra of Co_3O_4 nanoparticles.

The prepared Co_3O_4 material was further analyzed by a nitrogen desorption test. The isothermal curve of nitrogen absorption and desorption is shown in Figure 3a. The test results show that the specific surface area of the Co_3O_4 material is 146.6 m^2/g. Figure 3b

shows the pore size distribution curve of the material. The pore size distribution is more than 50 nm, and these pore sizes are formed by the interweaving of the materials. The large specific surface area of the material enables full contact between the electrolyte and the electrode material, accelerating the electrochemical reaction and improving the electrochemical performance [15].

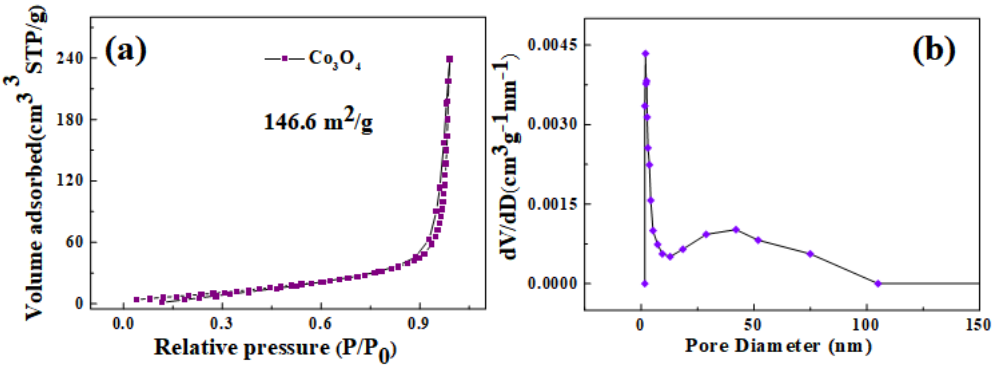

Figure 3. (**a**) Nitrogen adsorption-desorption isothermal curve. (**b**) Pore size distribution of Co_3O_4 nanosheets.

Electrochromic materials are a class of smart materials that can selectively absorb or transmit light to achieve color changes under electrical stimulation. They can reduce energy consumption, save energy, and adapt to the development of the times, so they are often used in energy-saving construction and intelligent transportation. In order to realize the industrialization of electrochromic devices, research on materials with excellent properties has become a current hotspot. Co_3O_4 is one of the widely used anode electrochromic materials [16].

Next, we gain a more accurate understanding of the electrochromic properties of the Co_3O_4 nanosheets by observing the transmittance and response time of the Co_3O_4 nanosheets. The transmittance and response time changes at a scan rate of 60 mV/s can be seen in Figure 4. The results show that the material has a transmission (ΔT of 75% at 780 nm. In the voltage range (from −1 to +1 V), the color of the Co_3O_4 changes. At a negative voltage, the Co_3O_4 was dyed yellow. After moving to a positive voltage, the film was bleached and returned to its original transparent state. The inset of Figure 4a shows the color change of the Co_3O_4. As shown in Figure 4b, the coloring response time and the bleaching response time is about 3.8 s and 3.4 s, respectively. The above experimental results show that the synthesized Co_3O_4 nanomaterials have high transmission contrast and short response time, as well as good electrochromic properties.

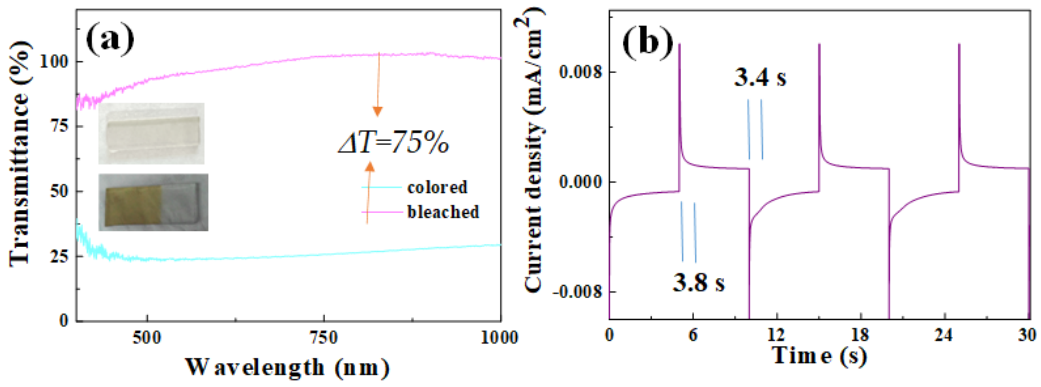

Figure 4. (**a**) Optical transmittance spectra of the Co_3O_4 nanomaterials. The inset shows the photographs of the Co_3O_4 nanomaterials in the colored and bleached states. (**b**) Switching response curves of the Co_3O_4 nanomaterials.

In the experiments, the electrochemical properties of the Co_3O_4 nanosheets were further analyzed. Figure 5a shows the CV curves of the Co_3O_4 nanosheets at different scan rates. There are a pair of obvious redox peaks in the CV curve, showing the pseudocapacitive properties of the material. The shape of the curve does not change significantly with an increasing scan rate. This indicates that the sheet-like structure of the Co_3O_4 electrode material has good stability. The figure shows that oxidation and reduction gradually peak with the increase of scan rate towards high potential and low potential, and tends to move slowly, showing that the oxidation-reduction process is a reversible reaction. In alkaline electrolytes, the main redox reaction equation is [17]:

$$Co_3O_4 + H_2O + OH^- \rightleftharpoons 3CoOOH + e^- \quad (5)$$

$$CoOOH + OH^- \rightleftharpoons CoO_2 + H_2O + e^- \quad (6)$$

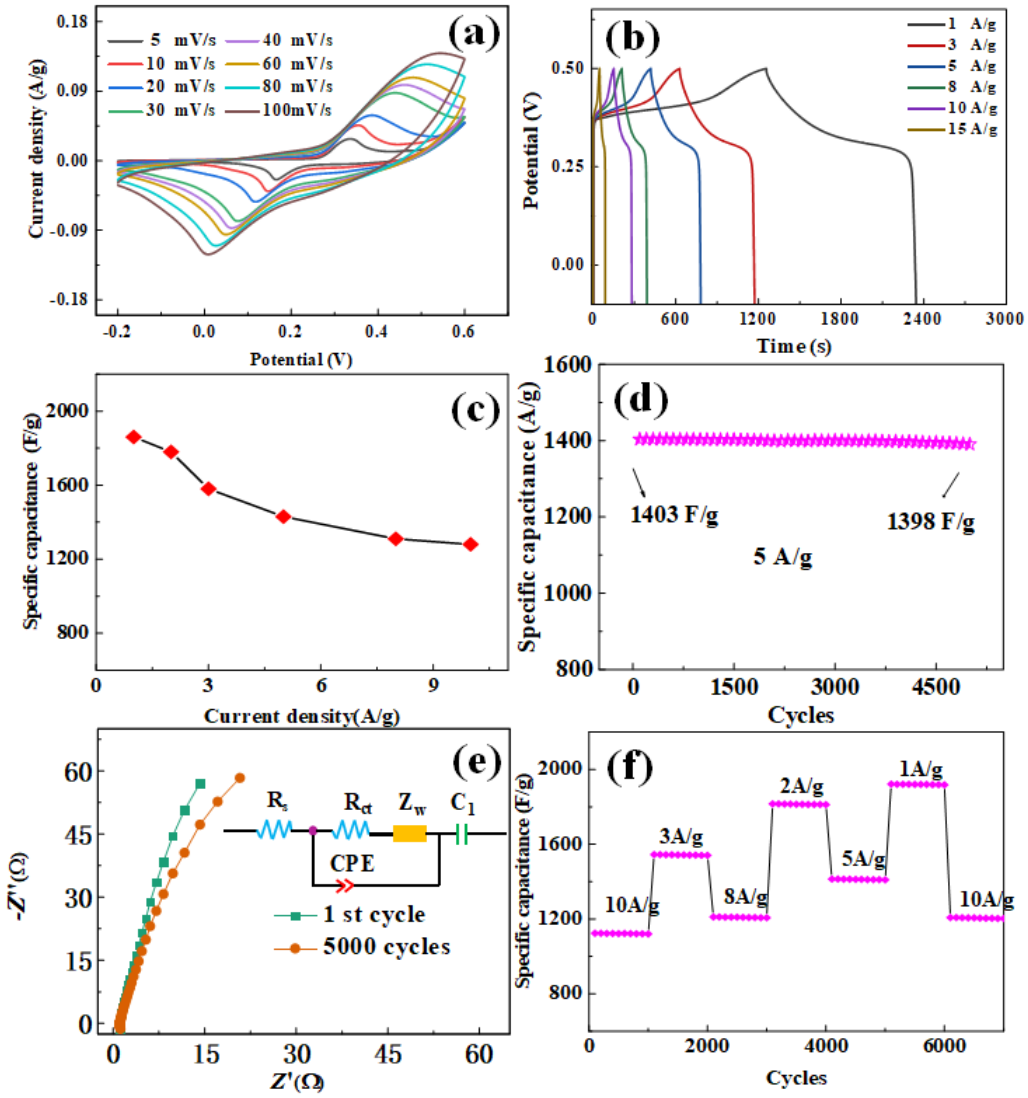

Figure 5. Electrochemical characterization of the Co_3O_4 nanosheets in a three−electrode system. (**a**) CV curves of Co_3O_4 nanosheets. (**b**) Charge-discharge curves of Co_3O_4 nanosheets at current densities of 1, 3, 5, 8, 10, and 15 A/g. (**c**) Specific capacitance of Co_3O_4 nanosheets at different current densities. (**d**) Cycle performance test of Co_3O_4 nanosheets at a current density of 5 A/g. (**e**) Nyquist diagram of the first cycle and after 5000 cycles of Co_3O_4 nanosheets. (**f**) Rate and cycle performance of the hybrid Co_3O_4 nanosheets under varied current densities.

Figure 5b shows the galvanostatic charge-discharge curves of the Co_3O_4 nanosheets at current densities of 1, 3, 5, 8, 10, and 15 A/g. We calculated the corresponding specific capacitance by Equation (1), as shown in Figure 5c. The results show that the specific capacitances of the electrodes at current densities of 1, 2, 3, 5, 8 and 10, A/g are 1850, 1786, 1583, 1403, 1374, and 1320 F/g, respectively. In order to better study the electrochemical stability of the Co_3O_4 nanosheets, we carried out charge-discharge cycle tests at a current density of 5 A/g. Figure 5d shows the variation curve of the specific capacitance of the Co_3O_4 sheet-like structure electrode and the number of cycles. After testing for 5000 cycles, the specific capacitance of the electrode decreased from 1403 to 1398 F/g and the capacitance retention rate reached 99.6%. The results show that the Co_3O_4 nanosheet electrode has good cycling stability. Figure 5e shows a comparison of the impedance of the Co_3O_4 nanosheet electrode material for the 1st and 5000th cycle. In the high-frequency region, the focal point of the curve on the solid axis, *Rs*, includes the internal impedance of the electroactive material, the ionic impedance of the electrolyte, and the contact impedance between the electrolyte and the surface of the electrode material [18]. The diameter of the semicircular arc reflects the electron transfer impedance, Rct. The inset shows the fitted equivalent circuit diagram. Warburg represents the diffusion of electrolytes in the electrode and the diffusion of protons in the host material [19]. The closer the straight line is to the imaginary axis, the lower the diffusion impedance is. The diffusion resistance of the material increased slightly after 5000 cycles, which may be due to the loss of active material after 5000 cycles and the inability of the material to fully react with the electrolyte [20]. We also carried out cycling stability experiments at different current densities. From Figure 5f, it can be seen that the specific capacitance of the sheet-like Co_3O_4 electrode material changes when the current density is continuously changed and then returned to the initial current density. The specific capacitance was consistently 1153 F/g during the first 1000 cycles, at a current density of 10 A/g. After continuously changing the current density and then returning to a current density of 10 A/g, the specific capacitance was 1195 F/g. This shows that the specific capacitance does not change significantly. The above results demonstrate the good electrochemical performance of the Co_3O_4 nanosheet electrode. Table 1 shows the electrochemical properties of Co_3O_4 nanomaterials and their comparison with the references. Here we also analyze and summarize the reasons for the good performance of the Co_3O_4 nanosheets. Firstly, the nanosheets interweave with each other to form a highly networked structure, creating a larger specific surface area and exposing more reactive sites, resulting in enhanced electrochemical performance. Secondly, we added surfactants (PEO-PPO-PEO) and a curing agent (hexamethylenetetramine) during the preparation process, which resulted in highly dispersed prepared materials and formed homogeneous Co_3O_4 nanosheets.

Table 1. The capacitance properties of the synthetic materials in this experiment are compared with those of the references.

Materials	Current Density [A/g]	Capacitance [F/g]	Number of Cycles	Retention [%]	Ref.
Co_3O_4	8	548	2000	98.5%	[21]
Co_3O_4/g-C_3N_4	1	1071	1000	95.5%	[22]
Co_3O_4	0.1	574	1000	95%	[23]
ZnO/Co_3O_4	1	1135	5000	83%	[24]
Co_3O_4	1	610	3000	94.5%	[25]
Co_3O_4/AC	0.1	491	5000	89%	[26]
Co_3O_4/CNT	2	406	10,000	93%	[27]
Co_3O_4@NiO-1	1	692.8	2500	90.88%	[28]
Co_3O_4@Ni_3S_2	1	1710	5000	83.5%	[29]
$CoMn_2O_4$@Co_3O_4	1	1627	5000	89.2%	[30]
Co_3O_4	1	1850	5000	99.6%	This paper

We further explored the electrochemical properties of the material by assembling an ASC device, using the Co_3O_4 nanoparticles electrode as the cathode, and the carbon nanotubes (CNTs) electrode as the cathode. As an ideal electrode material for supercapacitors, CNTs have excellent electrical conductivity and stable chemical properties. In this experiment, we prepared the CNTs by the chemical vapor deposition method. Before matching with the cathode material, we first performed charge-discharge tests on the CNTs electrode, as the anode, under different current densities. Figure 6 shows the charge-discharge test curves at current densities of 1, 3, 5, 8, 10, and 15 A/g, demonstrating the electric double-layer capacitance properties of the CNTs. Then we calculated the corresponding specific capacitance according to the specific capacitance calculation, using Equation (1). The specific capacitances of the electrodes at current densities of 1, 3, 5, 8, 10, and 15 A/g were 207, 198, 164, 143, 121, and 104 F/g, respectively. It can be seen that CNTs have stable electrochemical properties.

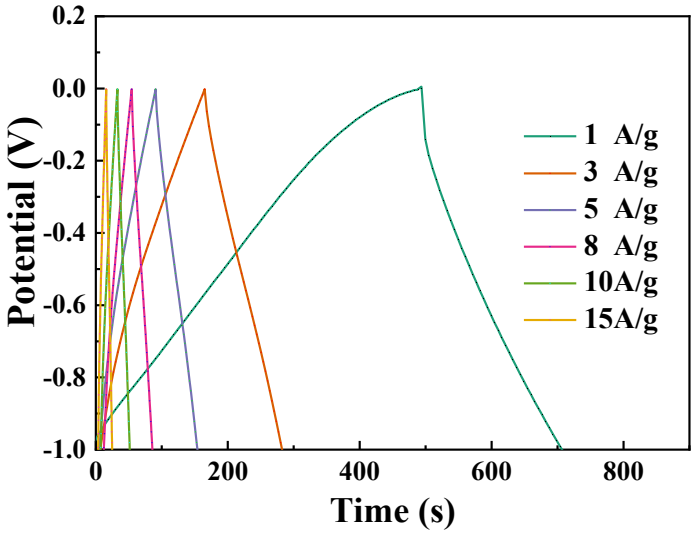

Figure 6. Charge-discharge test curves of the CNTs electrode for varied current densities.

During the experiment, the assembly of the device needs to match the quality of the positive and negative active materials. The specific capacitance of the negative and positive CNTs at 1 A/g were 207 and 1850 F/g, respectively, and the voltage changes were 1 and 0.5 V, respectively. According to Equation (4), the quality of the Co_3O_4//CNTs device of anode materials is $m^+/m^- \approx 1/5$. Next, we investigated the capacitive properties of the Co_3O_4//CNTs asymmetric device, as shown in Figure 7. The electrode CV curve of the test system is shown in Figure 7a, for anode material (Co_3O_4) and anode materials (CNTs) at a scanning speed of 20 mV/s while using 2 M KOH as the electrolyte. The potential window of Co_3O_4 was −1–0 V, and the potential window of the carbon nanotube electrode was −0.2–0.6 V. Figure 7b shows the CV curves of the Co_3O_4//CNTs device at potential windows of 0.8, 1.0, 1.2, 1.4, and 1.6 V. These CV curves all approximate parallelograms. From the figure, we can see the continuous change of different potential windows under the condition of a scanning speed of 15 mV/s. The shape of the CV curve does not change significantly when the potential window is 1.6 V, and there is no redundant precipitation peak, which indicates that the potential window of the Co_3O_4//CNTs device can be stabilized at 1.6 V. Therefore, subsequent research testing of Co_3O_4//CNTs asymmetric devices can be carried out with a research voltage window of 0–1.6 V to investigate their electrochemical properties. Figure 7c shows the CV curves of Co_3O_4//CNTs devices at scan speeds of 5, 20, 40, 60, 80, and 100 mV/s. It can be seen from the figure that the shape of the curve nearly does not change with the increase of the scanning speed, which verifies that the device has good electrochemical performance. The charge-discharge tests of the Co_3O_4//CNTs devices at different current densities are shown in Figure 7d. We calculated

the device under current densities of 1, 3, 5, 8, 10 and 15 A/g for specific capacitances of 339, 314, 307, 294, 287 and 278 F/g, respectively. The charging and discharging curves in the figure are basically symmetrical, reflecting the good capacitance performance of the device.

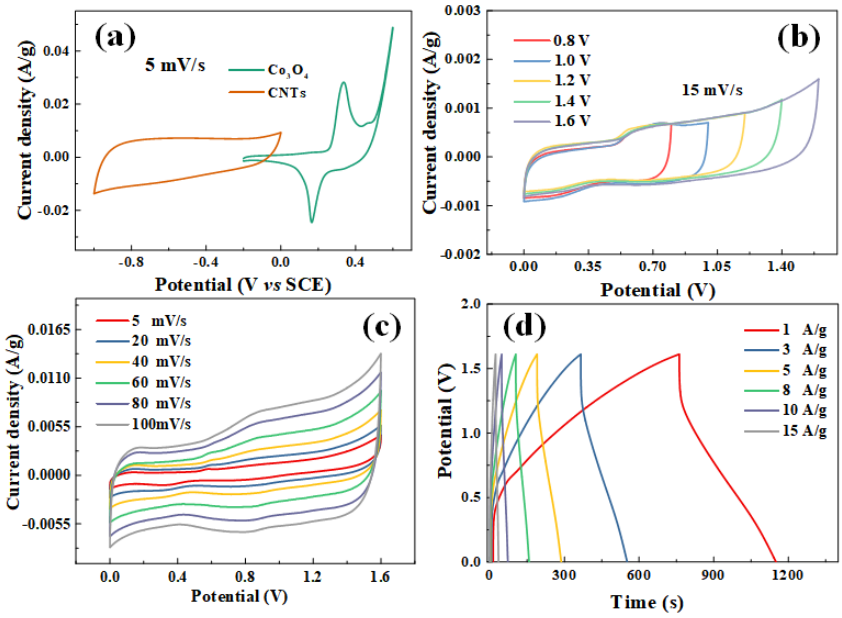

Figure 7. (**a**) CV curves of the hybrid Co_3O_4 electrode and CNTs electrodes in a three−electrode cell in a 2 M KOH electrolyte at a scan rate of 5 mV/s. (**b**) CV curves of the optimized Co_3O_4//CNTs device collected at different potential windows at a scan rate of 15 mV/s. (**c**) CV curves of Co_3O_4//CNTs devices at scanning speeds of 5, 20, 40, 60, 80, and 100 mV/s. (**d**) Charge and discharge tests of Co_3O_4//CNTs devices for varied current densities.

We compared our research work with other energy storage devices [31–34], as shown in Figure 8. According to the Equations (2) and (3), we calculated the Co_3O_4//CNTs device's energy density and power density. When the current density is 1 A/g, the power density of the device is 900 W/kg, and the maximum energy density is 79.52 Wh/kg. When the current density is 15 A/g, the maximum power density of the device is 11,000 W/kg, and even still, the energy density can reach 48.47 Wh/kg. By comparison, the performance of the Co_3O_4//CNTs device is significantly better than other energy storage devices listed in the literature.

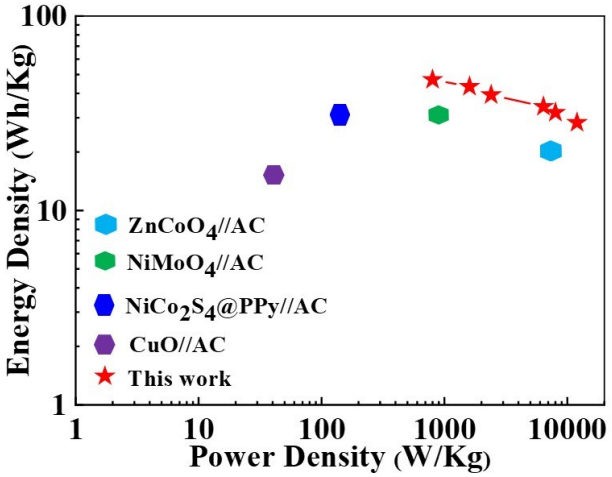

Figure 8. The Ragone plots relating power density to energy density of the asymmetric supercapacitor device [31–34].

4. Conclusions

In this paper, we successfully prepared Co_3O_4 nanosheets. According to the test results of SEM, XRD and TEM, the prepared materials are Co_3O_4 nanomaterials with sheet-like structures. In this paper, the electrochromic and capacitor properties of the prepared materials were investigated. The results show that the transmittance of Co_3O_4 nanosheets at 780 nm is close to 25% and 100%, in color and bleached states, respectively, and the modulation range of their transmittance to light is about 75%. The coloring response time and bleaching response time is about 3.8 s and 3.4 s, respectively. It can be seen that the synthetic material has good electrochromic properties. Electrochemical test results show that the specific capacitance of Co_3O_4 nanosheets reaches 1850 F/g when the current density is 1 A/g. When the current density is 5 A/g, after 5000 cycles, the specific capacitance retention rate is 99.6%, which shows good cycle stability and rate characteristics as a supercapacitor electrode material. In addition, the maximum voltage of the Co_3O_4//CNTs asymmetric device is 1.6 V, and it can provide a maximum energy density of 79.52 Wh/kg and a maximum power density of 11,000 W/kg, with excellent electrochemical performance. Devices such as these will play a more important role in areas such as the future of energy storage.

Author Contributions: X.Y. designed this experiment and carried out the experiments. G.W. wrote the manuscript and other analyses. G.W. and J.W. carried out the characterization tests, analyzed, wrote the results, and revised the manuscript. L.F., J.H., S.W. and M.Y. analyzed the characterization tests, wrote, and revised the manuscript. Y.L. analyzed and discussed the results. All authors have read and agreed to the published version of the manuscript.

Funding: This research work was supported by the Young Scientific Research Item of Harbin University of Commerce (18XN034), the National Natural Science Foundation of China (No. 52002099), the Foundation of State Key Laboratory of High-Efficiency Utilization of Coal and Green Chemical Engineering (Grant No. 2022-K74), and College Students' Innovative Entrepreneurial Training Plan Program (No. 202210240023).

Institutional Review Board Statement: Not applicable.

Informed Consent Statement: Not applicable.

Data Availability Statement: The data presented in this study are available in this article.

Conflicts of Interest: The authors declare no conflict of interests.

References

1. Muhammad, A.; Jatoi, A.S.; Mazari, S.A.; Abro, R.; Mubarak, N.M.; Ahmed, S.; Wahocho, S.A. Recent advances and developments in advanced green porous nanomaterial for sustainable energy storage application. *J. Porous Mater.* **2021**, *28*, 1945–1960. [CrossRef]
2. Lv, J.; Chen, J.; Lee, P.S. Sustainable wearable energy storage devices self-charged by human-body bioenergy. *SusMat* **2021**, *1*, 285–302. [CrossRef]
3. Zhou, Y.; Qi, H.; Yang, J.; Bo, Z.; Huang, F.; Islam, M.S.; Han, Z. Two-birds-one-stone: Multifunctional supercapacitors beyond traditional energy storage. *Energy Environ. Sci.* **2021**, *14*, 1854–1896. [CrossRef]
4. Guo, C.; Wang, H.; Liu, Y.; Zhang, Y.; Cui, S.; Guo, Z.; Ma, C. One-Dimensional/Two-Dimensional Homo-Orientation Co_3O_4/$NiCo_2O_4$ Nanoarray toward Ultrastable Hybrid Supercapacitor. *Energy Fuel* **2021**, *35*, 4524–4532. [CrossRef]
5. Yan, H.; Bai, J.; Liao, M.; He, Y.; Liu, Q.; Liu, J.; Wang, J. One-Step Synthesis of Co_3O_4/Graphene Aerogels and Their All-Solid-State Asymmetric Supercapacitor. *Eur. J. Inorg. Chem.* **2017**, *2017*, 1143–1152. [CrossRef]
6. Hu, X.; Wei, L.; Chen, R.; Wu, Q.; Li, J. Reviews and Prospectives of Co_3O_4-Based Nanomaterials for Supercapacitor Application. *ChemistrySelect* **2020**, *5*, 5268–5288. [CrossRef]
7. Zhou, Y.; Wang, Y.; Wang, J.; Lin, L.; Wu, X.; He, D. Controlled synthesis and characterization of hybrid Sn-doped Co_3O_4 nanowires for supercapacitors. *Mater. Lett.* **2018**, *216*, 248–251. [CrossRef]
8. Wang, N.; Liu, Q.; Kang, D. Facile self-cross-Linking cynthesis of 3D nanoporous Co_3O_4/carbon hybrid elec-trode materials for supercapacitors. *ACS Appl. Mater. Inter.* **2016**, *8*, 16035–16044. [CrossRef]
9. Wang, H.; Zhang, L.; Tan, X.; Holt, C.M.; Zahiri, B.; Olsen, B.C.; Mitlin, D. Supercapacitive properties of hydrothermally synthesized Co3O4 nanostructures. *J. Phys. Chem. C* **2011**, *115*, 17599–17605. [CrossRef]

10. Al-Jahdaly, B.A.; Abu-Rayyan, A.; Taher, M.M.; Shoueir, K. Phytosynthesis of Co_3O_4 Nanoparticles as the High Energy Storage Material of an Activated Carbon/Co_3O_4 Symmetric Supercapacitor Device with Excellent Cyclic Stability Based on a Na_2SO_4 Aqueous Electrolyte. *ACS Omega* **2022**, *7*, 23673–23684. [CrossRef]
11. Wang, L.; Song, X.C.; Zheng, Y.F. Electrochromic properties of nanoporous Co_3O_4 thin films prepared by electrodeposition method. *Micro Nano Lett.* **2012**, *7*, 1026–1029. [CrossRef]
12. Venkatesh, R.; Dhas, C.R.; Sivakumar, R.; Dhandayuthapani, T.; Sudhagar, P.; Sanjeeviraja, C.; Raj, A.M.E. Analysis of optical dispersion parameters and electrochromic properties of manganese-doped Co_3O_4 dendrite structured thin films. *J. Phys. Chem. Solids* **2018**, *122*, 118–129. [CrossRef]
13. Dhas, C.R.; Venkatesh, R.; Sivakumar, R.; Dhandayuthapani, T.; Subramanian, B.; Sanjeeviraja, C.; Raj, A.M.E. Electrochromic performance of chromium-doped Co_3O_4 nanocrystalline thin films prepared by nebulizer spray technique. *J. Alloys Compd.* **2019**, *784*, 49–59. [CrossRef]
14. Wang, J.; Wang, G.; Wang, S.; Hao, J.; Liu, B. Preparation of $ZnCo_2O_4$ Nanosheets Coated on evenly arranged and fully separated Nanowires with high capacitive and photocatalytic properties by a One-Step Low-Temperature Water bath method. *ChemistrySelect* **2022**, *7*, e202200472. [CrossRef]
15. Wang, K.; Zhao, C.G.; Min, S.D.; Qian, X.Z. Facile Synthesis of Cu_2O/RGO/$Ni(OH)_2$ Nanocomposite and Its Double Synergistic Effect on Supercapacitor Performance. *Electrochim. Acta* **2015**, *165*, 314–322. [CrossRef]
16. Yuan, C.; Li, M.; Wang, M.; Dan, Y.; Lin, T.; Cao, H.; Yang, H. Electrochemical development and enhancement of latent fingerprints on stainless steel via electrochromic effect of electrodeposited Co_3O_4 films. *Electrochim. Acta* **2021**, *370*, 137771. [CrossRef]
17. Xia, X.H.; Tu, J.P.; Zhang, Y.Q.; Mai, Y.J.; Wang, X.L.; Gu, C.D.; Zhao, X.B. Freestanding Co_3O_4 nanowire array for high performance supercapacitors. *Rsc. Adv.* **2012**, *2*, 1835–1841. [CrossRef]
18. Zhang, Y.; Cai, W.; Guo, Y.; Wang, Y. Self-supported Co-Ni-S@ CoNi-LDH electrode with a nanosheet-assembled core-shell structure for a high-performance supercapacitor. *J. Alloys Compd.* **2022**, *908*, 164635. [CrossRef]
19. Raj, C.J.; Manikandan, R.; Sivakumar, P.; Opar, D.O.; Savariraj, A.D.; Cho, W.J.; Kim, B.C. Origin of capacitance decay for a flower-like δ-MnO_2 aqueous supercapacitor electrode: The quantitative surface and electrochemical analysis. *J. Alloys Compd.* **2022**, *892*, 162199. [CrossRef]
20. Tian, Y.; Zhu, L.; Han, E.; Shang, M.; Song, M. Effect of templating agent on Ni, Co, Al-based layered double hydroxides for high-performance asymmetric supercapacitors. *Ionics* **2020**, *26*, 367–381. [CrossRef]
21. Meher, S.K.; Rao, G.R. Ultralayered Co_3O_4 for high-performance supercapacitor applications. *J. Phys. Chem. C* **2011**, *115*, 15646–15654. [CrossRef]
22. Chang, L.; Zhu, S.S.; Zhang, Y.J. Fabrication of supercapacitors using CO_3O_4/g-C_3N_4 nanomaterials and their electrochemical properties. *Mod. Chem.* **2021**, *41*, 107–111. [CrossRef]
23. Xu, J.; Gao, L.; Cao, J.; Wang, W.; Chen, Z. Preparation and electrochemical capacitance of cobalt oxide (Co_3O_4) nanotubes as supercapacitor material. *Electrochim. Acta* **2010**, *56*, 732–736. [CrossRef]
24. Gao, M.; Wang, W.K.; Rong, Q.; Jiang, J.; Zhang, Y.J.; Yu, H.Q. Porous ZnO-coated Co_3O_4 nanorod as a high-energy-density supercapacitor material. *ACS Appl. Mater. Inter.* **2018**, *10*, 23163–23173. [CrossRef]
25. Wang, X.; Xia, H.; Wang, X.; Gao, J.; Shi, B.; Fang, Y. Facile synthesis ultrathin mesoporous Co_3O_4 nanosheets for high-energy asymmetric supercapacitor. *J. Alloys Compd.* **2016**, *686*, 969–975. [CrossRef]
26. Zhou, F.Y.; Liu, Q.L.; Gu, J.J.; Zhang, W.; Zhang, D. A facile low-temperature synthesis of highly distributed and size-tunable cobalt oxide nanoparticles anchored on activated carbon for supercapacitors. *J. Power Source* **2015**, *273*, 945–953. [CrossRef]
27. Ramesh, S.; Haldorai, Y.; Sivasamy, A.; Kim, H.S. Nanostructured Co_3O_4/nitrogen doped carbon nanotube composites for high-performance supercapacitors. *Mater. Lett.* **2017**, *206*, 39–43. [CrossRef]
28. Wei, H.; Guo, X.; Wang, Y.; Zhou, Z.; Lv, H.; Zhao, Y.; Chen, Z. Inherently porous Co_3O_4@NiO core–shell hierarchical material for excellent electrochemical performance of supercapacitors. *Appl. Surf. Sci.* **2022**, *574*, 151487. [CrossRef]
29. Zhang, J.; Lin, J.; Wu, J.; Xu, R.; Lai, M.; Gong, C.; Chen, X.; Zhou, P. Excellent Electrochemical Performance Hierarchical Co_3O_4@Ni_3S_2 core/shell nanowire arrays for Asymmetric Supercapacitors. *Electrochim. Acta* **2016**, *207*, 87–96. [CrossRef]
30. Chen, X.B.; Liu, X.; Liu, Y.X.; Zhu, Y.M.; Zhuang, G.C.; Zheng, W.; Cai, Z.Y.; Yang, P.Z. Advanced binder-free electrodes based on $CoMn_2O_4$@Co_3O_4 core/shell nanostructures for high-performance supercapacitors. *RSC Adv.* **2018**, *8*, 31594–31602. [CrossRef]
31. Zhu, J.; Song, D.; Pu, T.; Li, J.; Huang, B.; Wang, W.; Chen, L. Two-dimensional porous $ZnCo_2O_4$ thin sheets assembled by 3D nanoflake array with enhanced performance for aqueous asymmetric supercapacitor. *Chem. Eng. J.* **2018**, *336*, 679–689. [CrossRef]
32. Moosavifard, S.E.; El-Kady, M.F.; Rahmanifar, M.S.; Kaner, R.B.; Mousavi, M.F. Designing 3D highly ordered nanoporous CuO electrodes for high-performance asymmetric supercapacitors. *ACS Appl. Mater. Inter.* **2015**, *7*, 4851–4860. [CrossRef] [PubMed]
33. Chen, S.; Yang, Y.; Zhan, Z.; Xie, J.; Xiong, J. Designed construction of hierarchical $NiCo_2S_4$@polypyrrole core–shell nanosheet arrays as electrode materials for high-performance hybrid supercapacitors. *RSC Adv.* **2017**, *7*, 18447–18455. [CrossRef]
34. Bandyopadhyay, P.; Saeed, G.; Kim, N.H.; Lee, J.H. Zinc-nickel-cobalt oxide@ $NiMoO_4$ core-shell nanowire/nanosheet arrays for solid state asymmetric supercapacitors. *Chem. Eng. J.* **2020**, *384*, 123357. [CrossRef]